New ESR dates from Lovedale, Free State, South Africa: implications for the study of tooth diagenesis

Maïlys Richard, Ifat Kaplan-Ashiri, Jesús Alonso María, Edwige Pons-Branchu, Arnaud Dapoigny, Lloyd Rossouw, Michael Toffolo

Field and Technical Report

NEW ESR DATES FROM LOVEDALE, FREE STATE, SOUTH AFRICA: IMPLICATIONS FOR THE STUDY OF TOOTH DIAGENESIS

MAÏLYS RICHARD[1]*, IFAT KAPLAN-ASHIRI[2], MARIA-JESUS ALONSO[3], EDWIGE PONS-BRANCHU[4], ARNAUD DAPOIGNY[4], LLOYD ROSSOUW[5,6] & MICHAEL B. TOFFOLO[1,3]

[1]*Archéosciences Bordeaux, UMR 6034 CNRS-Université Bordeaux Montaigne, Pessac, France*
*(*Corresponding author. Email: mailys.richard@u-bordeaux-montaigne.fr)*
[2]*Department of Chemical Research Support, Weizmann Institute of Science, Rehovot, Israel*
[3]*Geochronology and Geology Program, Centro Nacional de Investigación sobre la Evolución Humana (CENIEH), Burgos, Spain*
[4]*Laboratoire des Sciences du Climat et de l'Environnement, GEOTRAC-LSCE/IPSL, UMR 8212, CEA-CNRS-UVSQ, Université Paris-Saclay, Gif-sur-Yvette, France*
[5]*Florisbad Quaternary Research Department, National Museum Bloemfontein, Bloemfontein, South Africa*
[6]*Department of Plant Sciences, University of the Free State, Bloemfontein, South Africa*

(Received July 2023. Accepted August 2023)

ABSTRACT

Lovedale is the only open-air Middle Stone Age site in the Free State dated to early Marine Isotope Stage 4. Framing the chronology of this context, especially by taking into account diagenetic processes that may affect age results, is thus fundamental to understand modern human dynamics in the interior of South Africa. In a recent study, we investigated the effect of diagenesis on teeth samples collected for combined electron spin resonance and uranium-series dating at the site. By combining different characterisation methods, it was shown that the uranium (U) content of enamel varied in the specimens, and that it was positively correlated with the degree of crystallinity of carbonate hydroxyapatite, whereby larger amounts of U are associated with highly crystalline enamel. The large variability in U content was in contrast with the fact that teeth were found in the same depositional context. High levels of U in some of the samples limit the accuracy of age determinations, since several uncertainties remain regarding U uptake and leaching, which both affect dose rate modelling. In such complex cases, calculating minimum ages is the most cautious option. New samples were collected at the site during the excavation campaign in 2021. Enamel was analysed using Fourier transform infrared spectroscopy and scanning electron microscopy coupled with cathodoluminescence in order to determine its degree of atomic order and the presence of foreign ions (especially U), and the correlation between the two. We discuss here the contribution of U-uptake modelling on the age calculation, and present new ESR ages calculated assuming an early uptake of U, ranging from 84 ± 9 ka to 56 ± 5 ka. Together with previous ages obtained on the gravel layer, a weighted mean age of 64 ka can be used as a minimum age estimate for the base of the sequence.

Keywords: ESR, uranium series, U-uptake modelling, diagenesis, Middle Stone Age, Free State.

INTRODUCTION

Alluvial terraces in the Free State river catchments have produced several archaeological and palaeontological sites dated to the Pleistocene, which are often visible in section within natural erosional ravines, locally called dongas (Berger & Brink 1996; Brink *et al*. 1999; Brink & Rossouw 2000; Churchill *et al*. 2000; Brink 2004; Rossouw 2006; De Ruiter *et al*. 2011; Brink *et al*. 2012; Brink *et al*. 2016; Wroth *et al*. 2022; Bousman *et al*. 2023). In a region where organic remains suitable for radiocarbon dating are rarely preserved in sediments, dongas offer an exceptional opportunity to date archaeological and palaeontological occurrences *in situ* using trapped-charge dating methods, such as optically stimulated luminescence (OSL) of quartz and electron spin resonance (ESR) of tooth enamel (Lyons *et al*. 2014; Brink *et al*. 2016).

ESR dating, generally combined with U-series (ESR/U-series), is the only method available to date Pleistocene fossil teeth for periods beyond the range of radiocarbon, or in the absence of collagen. ESR is based on the capacity of the carbonate hydroxyapatite (HAP) of the enamel to record a dose of ionising rays, coming from the cosmic rays and the radioactive decay of natural isotopes, mainly uranium (U), thorium (Th) and potassium (K), present in the environment of the sample (sedimentary matrix, adjacent dental tissues) and the enamel itself. Due to the energy released, electrons are 'trapped' in defects of the crystal lattice. This process is a function of the irradiation dose received by the enamel during burial, allowing one to use this phenomenon for dating. Indeed, the dose absorbed in the HAP crystal can be quantified using ESR spectrometry (the equivalent dose, D_e), and the annual dose emitted in the environment and in the dental tissues (the dose rate, D_a) can be measured using different techniques (e.g. gamma spectrometry, mass spectrometry), with the ratio D_e/D_a providing the age. However, one of the main assumptions is that the D_a has been constant over time, and it is based on measurements that are conducted today. It is known that the kinetics of U-uptake in bones and teeth, which is soluble in water, can be complex and difficult to reconstruct. This is particularly true in the adjacent tissues of dentine and cement, which are more porous and whose composition is similar to bone mineral (*ca* 70% mineralised phase). Enamel, which exhibits a larger proportion of mineralised tissue, with *ca* 96% of HAP, is thus preferred for ESR dating. For samples where low levels of U are detected in the dental tissues (typically ≤1 ppm in dentine and cement, and <100 ppb in the enamel), the corresponding dose rate may be negligible (see examples in Richard *et al*. 2019). For those with high levels of U, which can reach several hundred ppm, the model used to reconstruct the dose rate is the main variable for the age calculation. Several models based on the measured U content have been developed in the past. The simplest one considers that U was incorporated

soon after burial, corresponding to an early uptake (EU); the linear uptake (LU) describes an equal increment of U per unit of time, and the recent uptake (RU) is based on a late U uptake. If a tooth has negligible U content in all dental tissues, the three models give the same age, considering the error range. Grün *et al*. (1988) proposed a model that allows taking into account not only the U content, but also the isotopic ratios commonly used for U-series dating ($^{234}U/^{238}U$ and $^{230}Th/^{234}U$). It is based on the calculation of the uptake parameter (the p-value), which is specific to each dental tissue, and can range from –1 (EU) to positive values (RU). This model is, however, limited to samples that did not suffer U loss (leaching) after burial, which is detected when at least one of the dental tissues has an apparent U-series age greater than the EU-ESR age of the tooth.

The U content in the dental tissues depends on different factors, such as the sedimentary and chemical environment of the sample, and its age. Lower levels are expected in the enamel (<1 ppm), while dentine and cement are more porous and thus contain more U. Furthermore, it also seems reasonable to assume that samples which belong to the same depositional context (same layer and square metre) have similar U content. However, in the case of the Middle Stone Age (MSA) site of Lovedale in the Free State (Fig. 1), previously dated samples had variable U content in the enamel, ranging from 1.7 to 29.6 ppm (Richard *et al*. 2022). Fourier transform infrared spectroscopy (FTIR) showed that the enamel samples that are richer in U are also the more diagenetically altered. Considering that enamel becomes more crystalline upon diagenesis in sediments (Weiner & Bar-Yosef 1990), whereby dissolution and reprecipitation processes produce larger and more ordered crystals at the atomic level, FTIR demonstrated that highly crystalline samples are primary candidates for U leaching. The five antelope teeth dated previously were collected from a gravel layer at the base of the stratigraphic sequence (Fig. 1), within the same square metre and at a similar elevation, raising questions about differential diagenesis at the microscale, which should be considered before processing samples for ESR/U-series dating. Despite such diversity in U content, the ages calculated assuming an early uptake of U all fall within the same range, from 63 ± 8 ka to 68 ± 15 ka, giving a weighted mean age of 64 ± 3 ka for the gravel layer (Richard *et al*. 2022). These ages were interpreted as minimum estimates, which are in agreement with OSL dates (Wroth *et al*. 2022).

In this article we present new ESR/U-series dates obtained from four teeth collected at Lovedale in 2021, in the same depositional context of the gravel layer. FTIR and SEM-CL analyses were performed in order to investigate the crystallinity and composition of the samples, and to provide

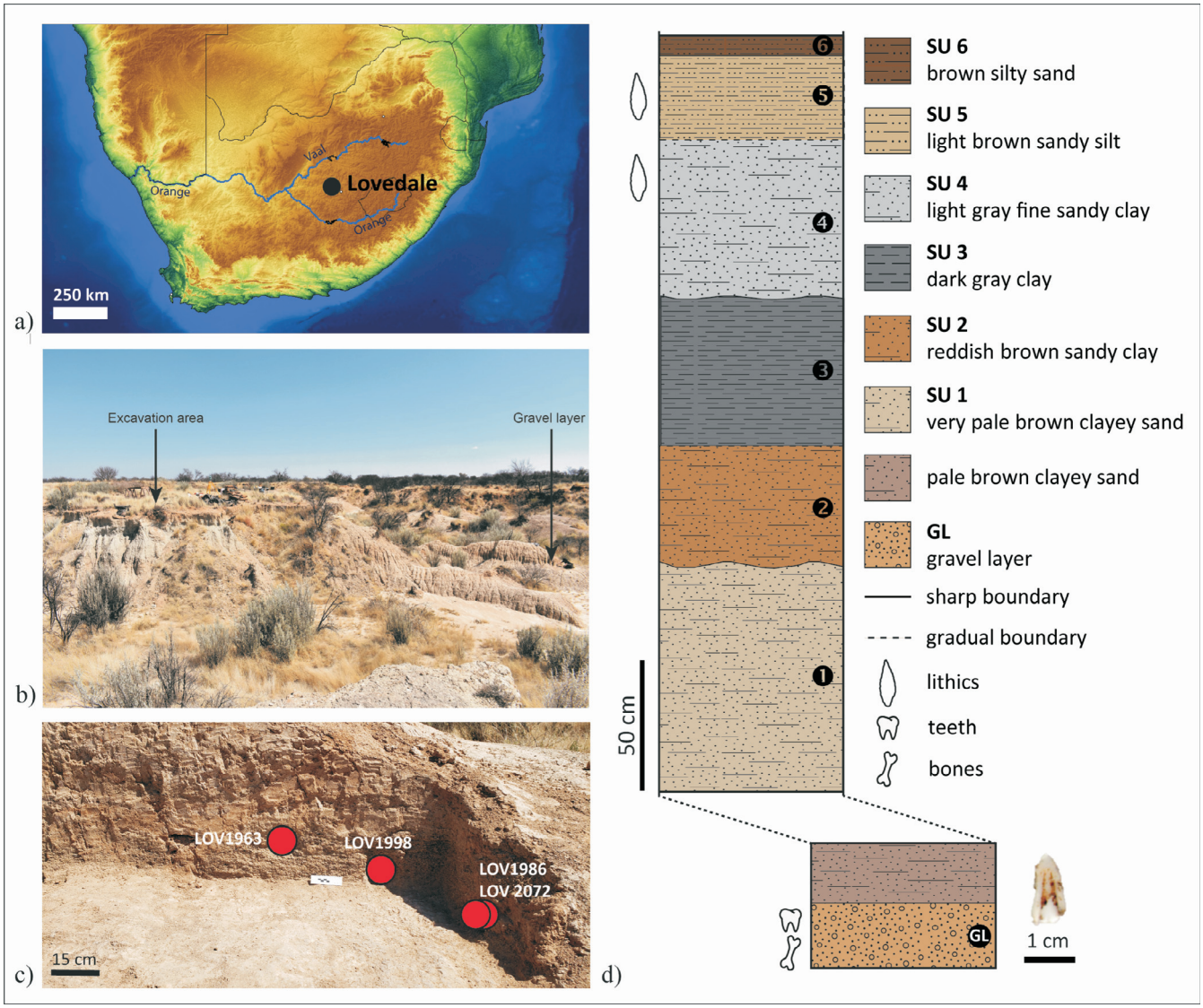

FIG. 1. (**a**) *Lovedale: location;* (**b**) *general view looking northwest;* (**c**) *view of the west section of the gravel layer and location of the gamma spectrometry measurements;* (**d**) *stratigraphic column with an example of one of the dated teeth (LOV 2072); SU: sedimentary unit.*

new insights into diagenetic processes that may affect the age calculation.

MATERIAL AND METHODS

SITE

Lovedale is located in a small donga on the left bank of the Modder River (28°54′2.35″S, 25°41′7.69″E, 1220 masl). The site features seven sedimentary units (SU), six of which occur in a single profile (numbered 1 to 6, from the base to the top), and an additional lens of gravel that was identified a few metres to the north of the main excavation area (Fig. 1). Geoarchaeological analyses have shown that sediments accumulated as a result of different flow regimes of the Modder, first as point bar deposits (gravel layer), and then as overbank sediments deposited by low-energy water. At different points in the sequence, land surface exposure favoured soil forming processes, as well as human occupation. The site has produced an MSA occupation dated to ~77–56 ka (top of SU4 and SU5), characterised by a pre-Howiesons Poort lithic industry on hornfels featuring many unifacial points that exhibit trimming of the base on both the dorsal and ventral sides, presumably for hafting. The large number of points in the lithic assemblage and the location next to a source of water clearly indicate that the site was related to hunting activities. The occurrence of ungulate fossils in the gravel layer, including the water-dependent species *Kobus leche* (lechwe), indicates that the site was part of the network of Florisian wetlands that punctuated the central interior of South Africa at different stages during the Pleistocene, which had the potential to sustain large animal populations and human groups (Brink 2016). The points from Lovedale, technologically reminiscent of the coeval Still Bay technocomplex found along the coast of South Africa, raise the issue of the relations between interior plateau and seaboard at the end of Marine Isotope Stage (MIS) 5 and during early MIS 4. At Lovedale, sediments from this period have yielded a large proportion of grass short cell phytoliths of the Chloridoideae subfamily, which reflect a locally dry climate, and thus reinforce the view that the river was a focal resource for human subsistence (Wroth *et al*. 2022).

The teeth dated by Richard *et al*. (2022) using ESR/U-series were collected in 2019 from the gravel layer at the base of the stratigraphic sequence. The excavation unit was expanded in 2021 and four additional teeth of an indeterminate small-sized ungulate, possibly *Antidorcas bondi* (Bond's springbok) as in the case of the 2019 samples, were recovered from the same square metre and elevation and selected for dating (Fig. 1).

FTIR

Teeth were analysed with FTIR at the CENIEH, Burgos (Spain), to determine their degree of atomic order based on the grinding curve method, whereby the full width at half maximum (FWHM) of the ν_3 band of phosphate is plotted against the infrared splitting factor (IRSF) (Fig. 2). The latter is obtained by dividing the sum of the intensity of the 604 and 565 cm^{-1} bands of phosphate by the intensity of the valley between them, and provides an indicator of crystallinity (Termine & Posner 1966; Weiner & Bar-Yosef 1990; Asscher, Regev *et al*. 2011; Asscher, Weiner *et al*. 2011). Plotting the IRSF with the FWHM allows control over particle size, and thus to separate the opposite effects of atomic order and particle size on the shape of infrared bands. Samples of enamel were powdered in an agate mortar and pestle and about 5 mg of each were mixed with 40 mg of KBr and pressed into 7-mm pellets using a hand press. Infrared spectra were collected in transmission mode after 32 scans within the 4000–400 cm^{-1} spectral range using a Thermo Scientific Nicolet iS5. Spectra were analysed using OMNIC 9.13 and Macros Basic 10 and compared to a modern *Antidorcas marsupialis* (springbok) reference (Richard *et al*. 2022). After analysis, the pellet was reground with greater vigour to reduce particle size, taking care, however, to discard half of the pellet prior to grinding to avoid overloading of the spectrum caused by increased surface absorption. The discarded half was replaced by KBr and pressed into a new pellet. This operation was repeated once more, so that we had three measurements for each sample.

SEM-CL

The cathodoluminescence (CL) of four samples (LOV2072, LOV1963, LOV1986, and LOV1998) was measured and analysed at the Department of Chemical Research Support, Weizmann Institute of Science, Rehovot (Israel). The emitted light lies mostly in the visible spectrum, but also in the near-infrared and ultraviolet range, excited by high-energy electrons from an electron beam in scanning electron microscopy (SEM). The SEM-CL measurements were performed with a

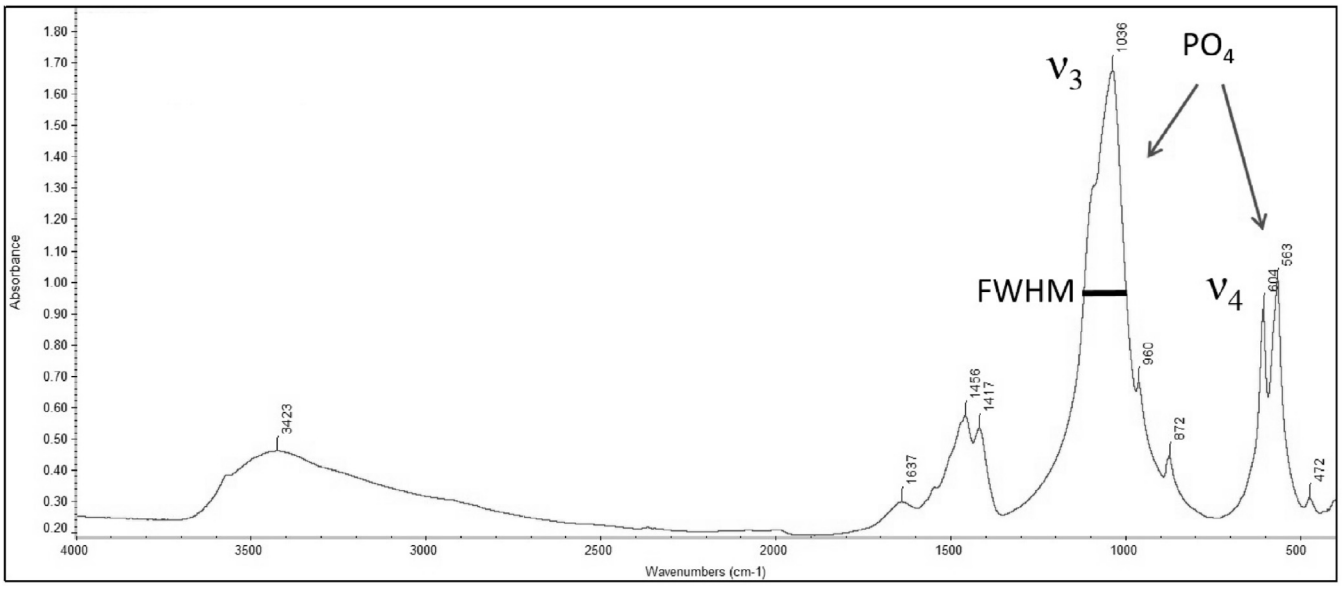

FIG. 2. *Representative FTIR spectrum of enamel carbonate hydroxyapatite. From Richard* et al. *(2022).*

Gatan MonoCL4 Elite system installed on a Zeiss GeminiSEM 500 high-resolution SEM. The luminescence was excited using an electron beam accelerated to 15 kV (with a 60 μm aperture). The collected light was directed to a monochromator with a spectral range of 200–1100 nm. The data were collected in Spectrum Imaging (SI) mode, where simultaneous SEM image and spectra were collected for a defined region of interest (ROI), allowing to correlate both the spectral information and electrons image. The SEM images were collected using the SE2 detector, and CL was acquired with the 150 lines/mm grating centred on 550 nm and 1 mm entrance slit. The spectrum images were acquired with a variable number of pixels (500–600 pixels) and with a pixel size in the range 2.4–7.7 μm. The exposure time was set to 2 s per pixel.

ESR AND U-SERIES DATING

ESR analyses were conducted at the CENIEH (Burgos, Spain). The teeth samples were composed of enamel and dentine, which were separated mechanically and cleaned using a dentist drill. The contribution of alpha rays (~20 μm) was removed from each side of the enamel (in contact with the dentine and the sediment) and the enamel was ground and sieved to ≤200 μm. The enamel powder (~50 mg) was divided into 11 aliquots (five for LOV1963 for which only ~30 mg of enamel was available) and irradiated at 40, 64, 100, 160, 250, 400, 640, 1000, 1600, and 2500 Gy (40, 100, 250, and 640 Gy for LOV1963), based on previous analyses (Richard *et al*. 2022). One aliquot was kept intact to measure the natural ESR signal. The ESR measurements were performed on a X-band spectrometer (Bruker EMXmicro-6/1) with the following parameters: 10–100 scans, 1 mW microwave power, 1024 points resolution, 10 mT sweep width, 100 kHz modulation frequency, 0.1 mT modulation amplitude, 20.48 ms conversion time and 5.12 ms time constant. The measurements were repeated three to five times, and the equivalent dose was calculated using the ESR intensity measured from the T1-B2 signal. Baseline correction (using a cubic function) and background subtraction (based on the peak heights measured over an average of 2 mT selected at the beginning and at the end of each spectrum) was applied (Fig. 3). The mean value of the ESR intensity calculated from the different series of measurements and associated standard deviations was plotted as a function of the irradiation dose using Origin Pro 8 (Origin Lab Corporation, Northampton, USA). Since the D_e values are inferior to 1000 Gy, the dose response curves were obtained by extrapolation using a single saturation exponential (SSE) function (Duval & Grün 2016) and weighted by the inverse of the squared ESR intensity ($1/I^2$).

U-series analyses were conducted at the LSCE (Gif-sur-Yvette, France). The dental tissues were dissolved in HNO_3 7M and spiked with a ^{229}Th-^{233}U-^{236}U solution calibrated against a Harwell Uraninite solution (HU-1), assumed to be at secular equilibrium. The chemical procedure for separation and purification of U and Th isotopes is described in Richard *et al*. (2015). Measurements were conducted using a multi-collector inductively coupled plasma mass spectrometer (MC-ICP-MS) (Thermo Scientific^{TM} Neptune Plus) fitted with a jet pump interface and a desolvating introduction system (aridus II) according to Pons-Branchu *et al*. (2014). U and Th fractions were combined for measurements: ^{238}U, ^{235}U, ^{236}U, ^{229}Th and ^{232}Th were measured on Faraday cups, ^{234}U and ^{230}Th on the ion counter (see details in Pons-Branchu *et al*. 2020).

The environmental dose rate includes the contribution of both beta and gamma dose from the sediment, and the cosmic rays. Each tooth was collected with embedding sediment. The sediment was used to measure U, Th, and K content with mass spectrometry, and derive the beta dose rate, after drying in an oven for one week at 40°C. The gamma dose rate was measured *in situ* using a portable gamma-ray multichannel analyser connected to a NaI (Tl) probe Inspector 1000 (Canberra) in the standing section, as close as possible to the initial location of each tooth. The data were treated following the threshold technique (Mercier & Falguères 2007). A water content of 15 ± 5% for the sediment was assumed based on previous OSL and ESR studies conducted at the site (Richard *et al*. 2022; Wroth *et al*. 2022). The cosmic dose rate was calculated from the equations of Prescott and Hutton (1988), considering a sediment cover of 4.6 ± 1 m (115 ± 13 μGy·a^{-1}).

Ages (1σ) were calculated using the DATA programme (Grün 2009), taking into account an alpha efficiency of 0.13 ± 0.02 (Grün & Katzenberger-Apel 1994), Monte Carlo beta

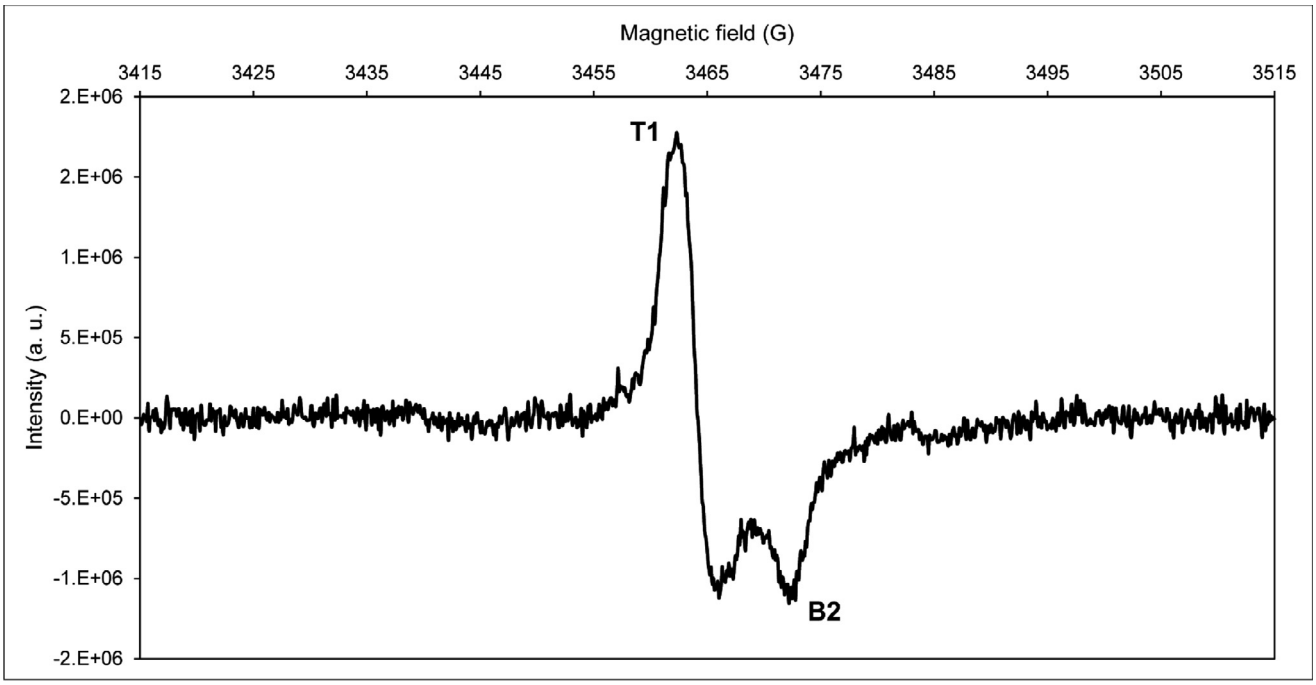

FIG. 3. *ESR spectrum of the natural aliquot of LOV2072 (100 scans, 3.7 mg).*

attenuation factors from Brennan *et al*. (1997), and a water content (weight %) of 0% for the enamel and of 7 ± 5% for the dentine. Equilibrium in the U-series decay chain was assumed in both sediment and dental tissues for the dose rate calculation.

RESULTS

CHARACTERISATION

The grinding curves of samples LOV1986 and LOV2072 overlap with the reference grinding curve of springbok. LOV1963 is slightly offset and runs above the springbok curve, indicating a mild degree of recrystallisation of carbonate hydroxyapatite. LOV1998 exhibits the largest offset, which is caused by extensive recrystallisation (Asscher, Regev *et al*. 2011) (Fig. 4).

The SEM-CL results are presented as true colour maps, where the colour of each pixel represents its spectral information, and also as spectra (single pixel spectrum or sum of the spectra measured for each region of interest) that are correlated with the SEM image. The CL true colour maps show a dominant purple-blue emission in all samples. Further SEM-CL analyses show that all samples exhibit bands at ~450 nm, characteristic of intrinsic defects in the crystal lattice of carbonate hydroxyapatite. While samples LOV2072, LOV1986, and LOV1998 show mainly an intense emission at 450 nm, sample LOV1963 exhibits detectable amounts of manganese and rare earth elements (REEs), represented by bands at 598 nm (Mn^{2+}), 643 nm (Sm^{3+}), and 486 and 573 nm (Dy^{3+}) (Ségalen *et al*. 2008) (Fig. 5). The purple emission is the dominant luminescence also in this sample as can be seen in the true colour map, but many pixels show lower intensity emission at 600 nm while others show the REEs.

DATING

The four dated teeth were collected in the same square metre (unit 9) and at the same depth (Z = 95), however, the equivalent doses differ greatly between samples (from 297 ± 21 Gy for LOV2072 to 530 ± 69 for LOV1998, Table 1 and Fig. 6). Note that S/N for the natural signals of the measured samples range from *ca* 26 (LOV1963) to 85 (LOV1998). LOV1963 and LOV1998 have the highest values of D_e, of 528 ± 50 Gy and 530 ± 69 Gy respectively that is correlated with high U content in the dental tissues, especially in the enamel (> 5 ppm). Consequently, their internal dose rate is up to 4 times higher than in the other two dated samples, LOV2072 and LOV1986, which have D_e of 297 ± 21 Gy and 339 ± 19 Gy, respectively. The environmental dose rate, i.e. the dose coming from the sediment around the samples and from the cosmic rays, has been calculated specifically for each sample using U, Th, and K contents for the beta dose rate and the values of *in situ* measurements for the gamma dose rate (Table 2). It is similar for all samples, with values ranging from 1252 ± 44 (LOV1998) to 1350 ± 53 μGy/a (LOV1963). The difference in the total dose rate lies in the U content in the dental tissues, unusually high in the enamel, with values ranging from 2.8 to 14 ppm, and reaching almost 200 ppm in the dentine (Table 3). Due to apparent U-series ages in some of the dental tissues older than the EU-ESR age of the tooth (Tables 1 & 3), the US-ESR model cannot be applied. We thus present here EU-ESR ages, with values ranging from 84 ± 9 ka (LOV1963) to 56 ± 5 ka (LOV2072), for the gravel layer at Lovedale.

DISCUSSION

As observed in previous samples (Richard *et al*. 2022), the degree of atomic order of carbonate hydroxyapatite determined by FTIR spectroscopy, which increases with diagenesis,

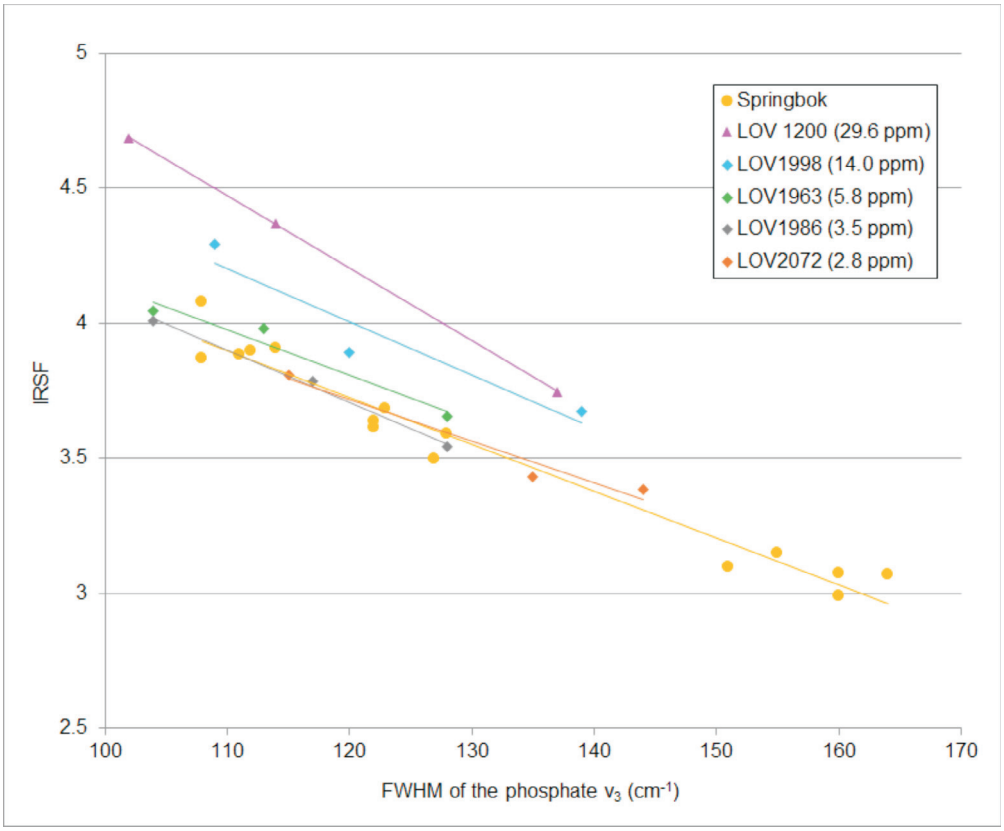

FIG. 4. *Grinding curve plot showing the degree of structural order of carbonate hydroxyapatite in the enamel of the Lovedale samples. Sample LOV1200 was analysed by Richard* et al. *(2022) and it is included as an example of extensively recrystallised enamel. IRSF: infrared splitting factor; FWHM: full width at half maximum. The grinding curves are represented by the trend lines.*

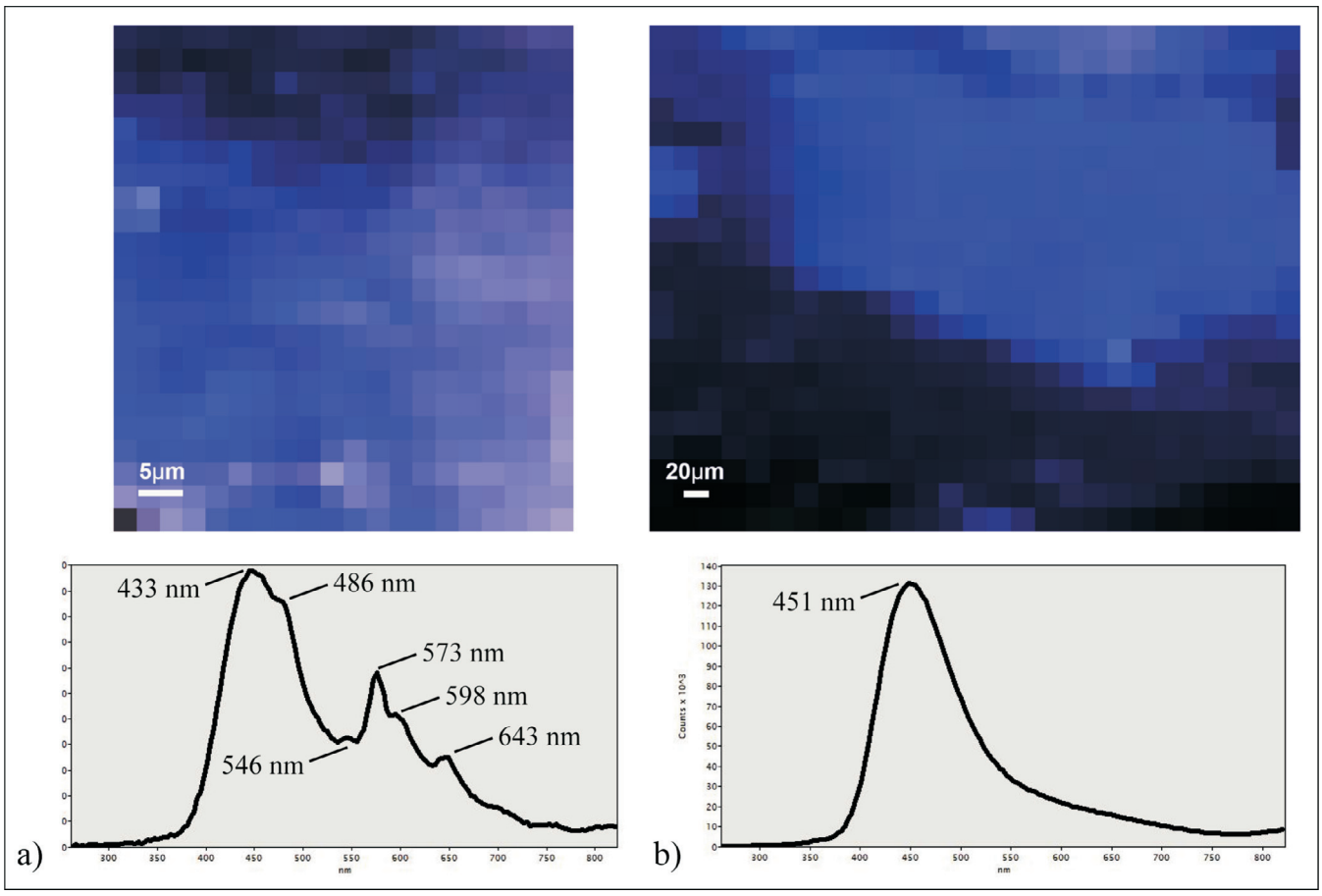

FIG. 5. *SEM-CL results obtained from LOV1963* (**a**) *and LOV1998* (**b**). *Top: colour map; bottom: spectrum showing the CL emission correlated to the SEM image. The emission bands at 430–450 nm represent intrinsic emission centres, such as lattice defects. According to Ségalen* et al. *(2008), the other emission bands can be correlated with* Mn^{2+} *(598 nm) and REEs such as* Dy^{3+} *(486 nm, 573 nm), and* Sm^{3+} *(643 nm). The 546 nm band might represent organic material.*

is correlated with the U content. The offset of the grinding curve of LOV2072 and LOV1986, with 2.77 ± 0.02 and 3.48 ± 0.03 ppm of U, respectively, falls in the range of the modern reference (springbok). However, LOV1963 is slightly shifted in comparison to the modern reference, for which a U content of 5.75 ± 0.05 ppm was measured. The larger offset is observed for LOV1998, which contains 13.98 ± 0.12 ppm of U. Based on all the data obtained on all the Lovedale teeth analysed to date (Richard *et al*. 2022, and this study), we are able to correlate preservation state and U content in the enamel using FTIR spectroscopy.

The SEM-CL results showed mainly the blue-purple emission band. The presence of U is expected to suppress the cathodoluminescence signal (Brigaud *et al*. 2021; Kennedy *et al*. 2023), but it was not observed. We were not able to identify U using SEM-CL, even in the enamel of LOV1998 which contains ~14 ppm (Table 3). This may be due to the very small amount of material used for the analyses. Pressed pellets with the same size can be used to compare also the intensity of the CL signal, but it was not possible to prepare them due to the small amount of material. Analyses on fragments, in the case of bigger teeth samples, may be more adapted to enamel in the future.

In general, in fossil teeth, U content in the enamel is lower than in the other tissues (< 1 ppm) and its contribution to the dose rate may be negligible (Richard *et al*. 2019). On the other hand, the dentine, which is more porous and less crystalline than the enamel, tends to incorporate higher contents of U, up to several hundred ppm, as it is the case of the Lovedale samples (Table 3). Moreover, if we consider apparent U-series ages (Table 3), they are in general older for the dentine than for the enamel, which may be interpreted as the effect of leaching, leading to an overestimation of the U-series age. Indeed, when

TABLE 1. *ESR/U-series dating results (1σ). The beta dose rate was derived from U, Th, and K content measured in the sediment (see Table 2). The gamma dose rate was measured* in situ *and a sediment thickness covering the samples of 4.6 ± 1 m was considered for the cosmic dose rate. U-uptake was reconstructed using the EU model (see data in Table 3). A water content (weight %) of 15 ± 5% for the sediment, of 0% for the enamel, and of 7 ± 5% for the dentine were assumed. Adj.* r^2 *is the adjusted coefficient of determination and express the quality of the fitting of the dose response curve.*

LOV #	D_e (Gy)	Adj. r^2	Dose rate (µGy/a)					EU-ESR age (ka)
			Enamel ($\alpha+\beta$)	Dentine (β)	Sediment (β)	Sediment (γ + cosmic)	Total	
2072	297 ± 21	0.995	960 ± 115	3156 ± 250	249 ± 31	987 ± 24	5347 ± 278	56 ± 5
1963	528 ± 50	0.999	2140 ± 245	2793 ± 220	354 ± 41	996 ± 34	6283 ± 333	84 ± 9
1986	339 ± 19	0.997	1243 ± 145	2463 ± 199	271 ± 32	987 ± 34	4964 ± 250	68 ± 5
1998	530 ± 69	0.985	4672 ± 468	2641 ± 255	204 ± 27	1048 ± 34	8565 ± 535	62 ± 9

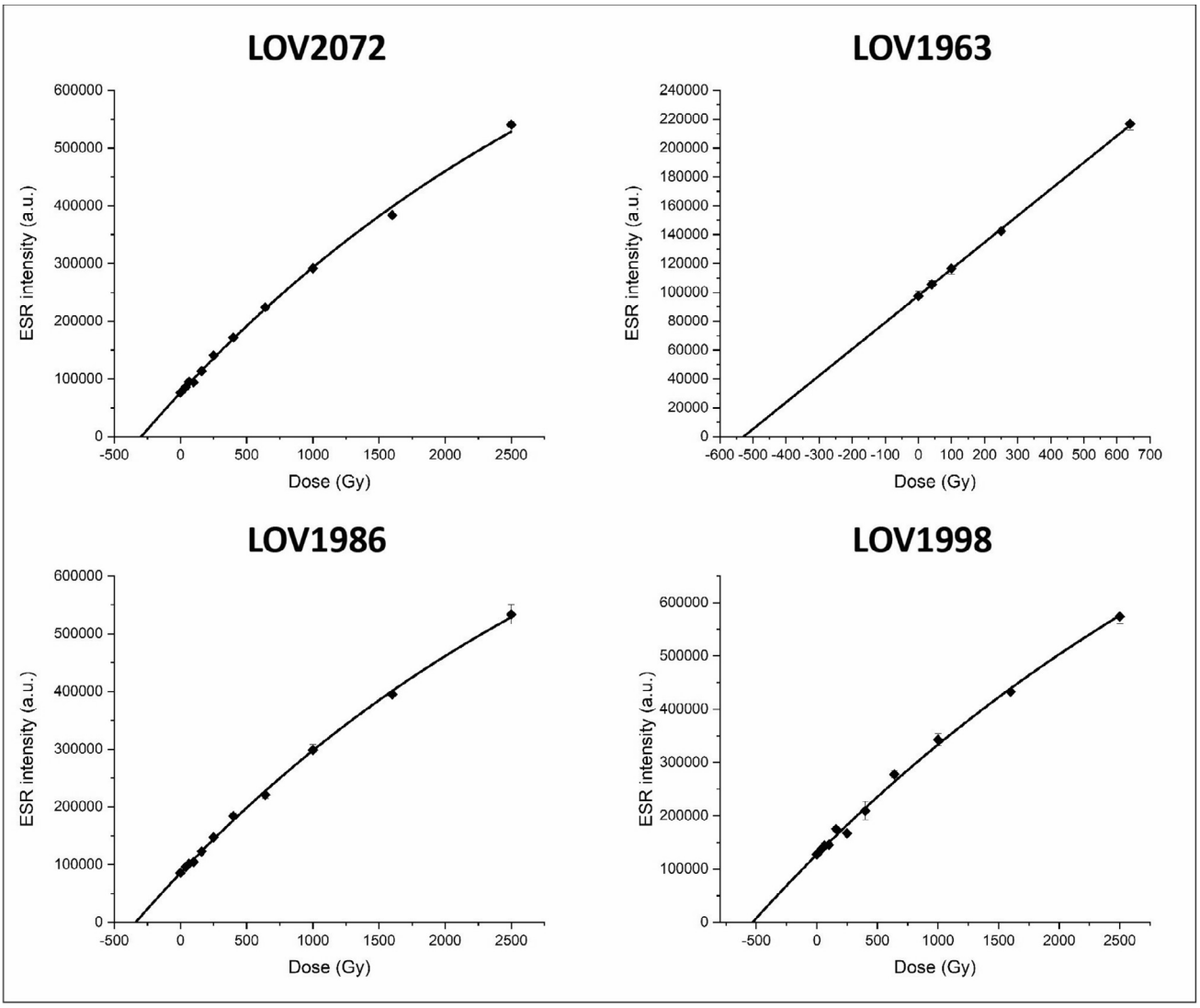

FIG. 6. *Dose response curves obtained for the Lovedale samples.*

at least one of the tissues in a tooth has a U-series age that is older than the mean ESR age calculated in DATA, no calculation is possible using the US-ESR model (Grün 2009). This is the main limitation encountered here. For this reason, we decided to present ages calculated assuming an early uptake of uranium (EU-ESR). Such a model will produce the highest dose rate possible coming from the dental tissue, since U is considered to be incorporated soon after burial and gives a minimum age.

The unusual high U content in the enamel of the Lovedale teeth, of more than 2 ppm, produces by its own 18% (LOV2072) to 55% (LOV1998) of the total dose rate calculated using the EU model, since both alpha and beta rays must be taken into account for the internal dose rate. If we add the contribution of the dentine, the dental tissues contribute from 75% (LOV1986) to 85% (LOV1998) to the total dose rate. The environmental dose rate (sediment + cosmic rays) represents less than a quarter of the dose rate. Thus, the EU-ESR ages presented here rely mainly on the presence of uranium in the dental tissues, and must be interpreted as minimum age estimates, considering the issues mentioned above. We should keep in mind that the older age of 84 ± 9 ka obtained for LOV1963 was calculated using a D_e value extrapolated from five experimental points instead of 11 for the other samples, and using a D_{max} of 640 Gy, which is 1.2*D_e (instead of ~5*D_e following the recommendations of Duval and Grün [2016] for the evaluation of reliable D_e). An overestimation of the D_e in that case cannot be excluded, thus leading to an age overestimate.

TABLE 2. *U, Th, and K content from the sediment samples containing the teeth, determined using mass spectrometry and used to derive the beta dose rate,* in situ *gamma dose rate and enamel thickness used to calculate the beta attenuation (side 1 = internal dentine; side 2 = sediment); LOV2072 and LOV1986 were found in the same spot, and therefore one* in situ *measurement was performed for the two (see Fig. 1).*

LOV #	U (ppm)	Th (ppm)	K (%)	*In-situ* γ dose rate (μGy/a)	Enamel thickness (μm)		
					Initial	Side 1	Side 2
2072	2.86 ± 0.20	7.72 ± 0.77	1.48 ± 0.10	872 ± 31	670	40	59
1963	3.66 ± 0.26	8.06 ± 0.81	1.50 ± 0.11	881 ± 31	468	20	35
1986	2.77 ± 0.19	6.81 ± 0.68	1.47 ± 0.10	872 ± 31	631	20	20
1998	2.90 ± 0.20	8.23 ± 0.82	1.53 ± 0.11	933 ± 32	964	20	20

TABLE 3. *U-series results. Apparent ages (2σ) are not used in the age calculation but are provided for each dental tissue for information.*

LOV #	Tissue	Labcode	[^{238}U] ppm	[^{232}Th] ppb	(^{234}U/^{238}U)	(^{230}Th/^{234}U)	(^{230}Th/^{232}Th)	Apparent age (ka)
2072	E	10287	2.77 ± 0.02	11.27 ± 0.09	2.2653 ± 0.0037	0.4926 ± 0.0013	828 ± 2	68.973 ± 0.251
	D	10003	178.67 ± 1.48	165.62 ± 1.68	2.3661 ± 0.0036	0.5953 ± 0.0043	5069 ± 36	107.872 ± 1.188
1963	E	10286	5.75 ± 0.05	132.02 ± 1.06	2.0006 ± 0.0022	0.6134 ± 0.0011	162 ± 1	94.086 ± 0.268
	D	10005	112.33 ± 0.90	10.40 ± 0.13	2.1075 ± 0.0031	0.7136 ± 0.0070	54393 ± 527	89.003 ± 1.031
1986	E	10288	3.48 ± 0.03	18.41 ± 0.15	2.0766 ± 0.0020	0.5908 ± 0.0015	701 ± 2	88.864 ± 0.361
	D	10004	127.27 ± 1.03	140.76 ± 1.46	2.1835 ± 0.0022	0.6754 ± 0.0044	4448 ± 29	112.752 ± 1.589
1998	E	10289	13.98 ± 0.12	11.26 ± 0.19	1.9354 ± 0.0033	0.5956 ± 0.0088	4675 ± 69	90.424 ± 2.031
	D	10006	197.59 ± 1.62	74.89 ± 0.79	1.9625 ± 0.0030	0.6900 ± 0.0054	11933 ± 91	116.335 ± 1.803

In total, nine ESR dates have been obtained for the gravel layers at Lovedale. Combining previous and new ages, we are able to propose a weighted mean age of 64 ± 2 ka (calculated with a weight of $1/\sigma^2$), as a minimum age estimate for the base of the sequence (63 ± 2 ka, excluding LOV1963). This age, in agreement with previous OSL dates, corroborates the interpretation that the sedimentary sequence exposed at the Lovedale donga accumulated in a relatively short period of time between the end of MIS 5 and the end of MIS 4 (Wroth *et al*. 2022).

CONCLUSIONS

The new analyses conducted on tooth enamel confirmed the chronology of the Lovedale sequence, which was deposited between the end of MIS 5 and the end of MIS 4 according to both ESR and OSL ages (Richard *et al*. 2022; Wroth *et al*. 2022). They also support the hypothesis according to which differential diagenesis occurred at the microscale, leading to variation in the degree of preservation between the teeth samples (Richard *et al*. 2022). Considering the high U content in most of the dental tissues, the age calculation relies mainly on the choice of the model used for U-uptake and dose rate reconstruction. Based on previously analysed samples, a weighted mean age of 64 ka is proposed as a minimum estimate for the gravel layer. Further investigations must be conducted in the future to better understand the diagenetic processes that affect the age resolution for ESR dating, and select the best-preserved samples that contain low U content, and that did not suffer U loss during burial.

ACKNOWLEDGEMENTS

Excavations at Lovedale were funded by a grant from the Deutsche Forschungsgemeinschaft (n. MI 1748/4-1) to C.E. Miller (University of Tübingen). M.B. Toffolo was funded by a grant from IdEx Bordeaux (grant n. ANR-10-IDEX-03-02), and by the grant RYC2021-030917-I funded by the MCIN/AEI/10.13039/501100011033 and by the European Union NextGenerationEU/PRTR. Archaeological excavations at Lovedale were conducted under the auspices of the National Museum Bloemfontein, with a permit from the South African Heritage Resources Agency (permit ID 2862 to L. Rossouw and M. Toffolo). We thank PANOPLY (Plateforme analytique géosciences Paris-Saclay) for the use of the MC-ICPMS and M. Duval (CENIEH) for his help with sediment mass spectrometry. Many thanks to F. du Toit for allowing excavations at the Lovedale Farm. Finally, we thank the two reviewers for their comments, which improved the manuscript.

REFERENCES

Asscher, Y., Regev, L., Weiner, S. & Boaretto, E. 2011. Atomic disorder in fossil tooth and bone mineral: an FTIR study using the grinding curve method. *ArcheoSciences* 35: 135–141.

Asscher, Y., Weiner, S. & Boaretto, E. 2011. Variations in atomic disorder in biogenic carbonate hydroxyapatite using the infrared spectrum grinding curve method. *Advanced Functional Materials* 21(17): 3308–3313.

Berger, L.R. & Brink, J. 1996. Late Middle Pleistocene fossils, including a human patella, from the Riet River gravels, Free State, South Africa. *South African Journal of Science* 92(6): 277–278.

Bousman, C.B., Brink, J.S., Rossouw, L., Bateman, M.D., Morris, S.E., Meier, H., Cohen, B., Trower, G., Herries, A.I.R., Palmison, M., Ringstaff, C., Thornton-Barnett, S. & Dworkin, S. 2023. Erfkroon: Late Quaternary alluvial geology, paleoenvironments and Stone Age archaeology in the western Free State, South Africa. In: Beyin, A., Wright, D.K., Wilkins, J., Bouzouggar, A. & Olszewski, D.I. (eds) *Handbook of Pleistocene Archaeology of Africa: Hominin Behavior, Geography, and Chronology*: 1431–1450. Springer International Publishing.

Brennan, B.J., Rink, W.J., McGuirl, E.L., Schwarcz, H.P. & Prestwich, W.V. 1997. Beta doses in tooth enamel by "one-group" theory and the ROSY ESR dating software. *Radiation Measurements* 27(2): 307–314.

Brigaud, B., Andrieu, S., Blaise, T., Haurine, F. & Barbarand, J. 2021. Calcite uranium–lead geochronology applied to hardground lithification and sequence boundary dating. *Sedimentology* 68(1): 168–195.

Brink, J.S. 2004. The taphonomy of an Early/Middle Pleistocene hyaena burrow at Cornelia-Uitzoek, South Africa. *Revue de Paléobiologie* 23(2): 731–740.

Brink, J.S. 2016. Faunal evidence for a mid- and late Quaternary environmental change in southern Africa. In: Knight, J. & Grab, S.W. (eds) *Quaternary Environmental Change in Southern Africa: Physical and Human Dimensions*: 284–305. Cambridge: Cambridge University Press.

Brink, J.S., Berger, L.R. & Churchill, S.E. 1999. Mammalian fossils from erosional gullies (dongas) in the Doring River drainage, central Free State, South Africa. In: Berger, C., Manhart, H., Peters, J. & Schibler, J. (eds) *Historia animalium ex ossibus: Beiträge zur Paläoanatomie, Archäologie, Ägyptologie, Ethnologie und Geschichte der Tiermedizin: Festschrift für Angela von den Driesch*: 79–90. Rahden/Westfalen: Verlag Marie Leidorf.

Brink, J.S., Bousman, C.B. & Grün, R. 2016. A reconstruction of the skull of *Megalotragus priscus* (Broom 1909), based on a find from Erfkroon, Modder River, South Africa, with notes on the chronology and biogeography of the species. *Palaeoecology of Africa* 33: 71–94.

Brink, J.S., Herries, A.I.R., Moggi-Cecchi, J., Gowlett, J.A.J., Bousman, C.B., Hancox, J.P., Grün, R., Eisenmann, V., Adams, J.W. & Rossouw, L. 2012. First hominine remains from a ~1.0 million year old bone bed at Cornelia-Uitzoek, Free State Province, South Africa. *Journal of Human Evolution* 63: 527–535.

Brink, J.S. & Rossouw, L. 2000. New trial excavations at the Cornelia-Uitzoek type locality. *Navorsinge van die Nasionale Museum Bloemfontein* 16: 141–156.

Churchill, S.E., Brink, J.S., Berger, L.R., Hutchinson, R.A., Rossouw, L., Stynder, D., Hancox, P.J., Brandt, D., Woodborne, S., Loock, J.C., Scott, L. & Ungar, P. 2000. Erfkroon: a new Florisian fossil locality from fluvial contexts in the western Free State, South Africa. *South African Journal of Science* 96: 161–163.

De Ruiter, D.J., Churchill, S.E., Brophy, J.K. & Berger, L.R. 2011. Regional survey of Middle Stone Age fossil vertebrate deposits in the Virginia-Theunissen area of the Free State, South Africa. *Navorsinge van die Nasionale Museum Bloemfontein* 27: 1–20.

Duval, M. & Grün, R. 2016. Are published ESR dose assessments on fossil tooth enamel reliable? *Quaternary Geochronology* 31: 19–27.

Grün, R. 2009. The DATA program for the calculation of ESR age estimates on tooth enamel. *Quaternary Geochronology* 4: 231–232.

Grün, R. & Katzenberger-Apel, O. 1994. An alpha irradiator for ESR dating. *Ancient TL* 12(2): 35–38.

Grün, R., Schwarcz, H.P. & Chadam, J. 1988. ESR dating of tooth enamel: coupled correction for U-uptake and U-series disequilibrium. *International Journal of Radiation Applications and Instrumentation*. *Part D. Nuclear Tracks and Radiation Measurements* 14(1–2): 237–241.

Kennedy, A.K., Wotzlaw, J-F., Crowley, J.L., Schmitz, M., Schaltegger, U., Wade, B., Martin, L., Talavera, C., Ware, B. & Bui, T.H. 2023. Apatite reference materials for SIMS microanalysis of isotopes and trace elements. *Geostandards and Geoanalytical Research* 47(2): 373–402.

Lyons, R., Tooth, S. & Duller, G.A.T. 2014. Late Quaternary climatic changes revealed by luminescence dating, mineral magnetism and diffuse reflectance spectroscopy of river terrace palaeosols: a new form of geoproxy data for the southern African interior. *Quaternary Science Reviews* 95: 43–59.

Mercier, N. & Falguères, C. 2007. Field gamma dose-rate measurement with a NaI(Tl) detector: re-evaluation of the "threshold" technique. *Ancient TL* 25(1): 1–4.

Pons-Branchu, E., Douville, E., Roy-Barman, M., Dumont, E., Branchu, P., Thil, F., Frank, N., Bordier, L. & Borst, W. 2014. A geochemical perspective on Parisian urban history based on U–Th dating, laminae counting and yttrium and REE concentrations of recent carbonates in underground aqueducts. *Quaternary Geochronology* 24: 44–53.

Pons-Branchu, E., Sanchidrián, J.L., Fontugne, M., Medina-Alcaide, M.Á., Quiles, A., Thil, F. & Valladas Sanchidrián, H. 2020. U-series dating at Nerja cave reveal open system. Questioning the Neanderthal origin of Spanish rock art. *Journal of Archaeological Science* 117: 105–120.

Prescott, J.R. & Hutton, J.T. 1988. Cosmic ray and gamma ray dosimetry for TL and ESR. *International Journal of Radiation Applications and Instrumentation Part D. Nuclear Tracks and Radiation Measurements* 14: 223–227.

Richard, M., Falguères, C., Pons-Branchu, E., Bahain, J.J., Voinchet, P., Lebon, M., Valladas, H., Dolo, J.M., Puaud, S., Rué, M., Daujeard, C., Moncel, M.H. & Raynal, J.P. 2015. Contribution of ESR/U-series dating to the chronology of late Middle Palaeolithic sites in the middle Rhône valley, southeastern France. *Quaternary Geochronology* 30: 529–534.

Richard, M., Falguères, C., Valladas, H., Ghaleb, B., Pons-Branchu, E., Mercier, N., Richter, D. & Conard, N.J. 2019. New electron spin resonance (ESR) ages from Geißenklösterle Cave: a chronological study of the Middle and early Upper Paleolithic layers. *Journal of Human Evolution* 133: 133–145.

Richard, M., Pons-Branchu, E., Carmieli, R., Kaplan-Ashiri, I., Alvaro Gallo, A., Ricci, G., Caneve, L., Wroth, K., Dapoigny, A., Tribolo, C., Boaretto, E. & Toffolo, M.B. 2022. Investigating the effect of diagenesis on ESR dating of Middle Stone Age tooth samples from the open-air site of Lovedale, Free State, South Africa. *Quaternary Geochronology* 69: 101269.

Rossouw, L. 2006. Florisian mammal fossils from erosional gullies along the Modder River at Mitasrust farm, central Free State, South Africa. *Navorsinge van die Nasionale Museum Bloemfontein* 22: 145–161.

Ségalen, L., de Rafélis, M., Lee-Thorp, J.A., Maurer, A-F. & Renard, M. 2008. Cathodoluminescence tools provide clues to depositional history in Miocene and Pliocene mammalian teeth. *Palaeogeography, Palaeoclimatology, Palaeoecology* 266: 246–253.

Termine, J.D. & Posner, A.S. 1966. Infrared analysis of rat bone: age dependency of amorphous and crystalline mineral fractions. *Science* 153(3743): 1523–1525.

Weiner, S. & Bar-Yosef, O. 1990. States of preservation of bones from prehistoric sites in the Near East: a survey. *Journal of Archaeological Science* 17(2): 187–196.

Wroth, K., Tribolo, C., Bousman, C.B., Horwitz, L.K., Rossouw, L., Miller, C.E. & Toffolo, M.B. 2022. Human occupation of the semi-arid grasslands of South Africa during MIS 4: new archaeological and paleoecological evidence from Lovedale, Free State. *Quaternary Science Reviews* 283: 107455.